7th IFToMM-Conference on Rotor Dynamics, Vienna, Austria, 25-28 September 2006

Investigation of a Rotordynamic Instability in a High Pressure Centrifugal Compressor Due to Damper Seal Clearance Divergence

J. Jeffrey Moore, Ph.D.
Southwest Research Institute®
Mechanical & Materials
Engineering Division
6220 Culebra Road
San Antonio, TX 78238 USA
jeff.moore@swri.org

Massimo Camatti
GE Oil & Gas, Nuovo Pignone
Via Felice Matteucci, 2
50127 Florence, Italy
massimo.camatti@np.ge.com

Anthony J. Smalley, Ph.D.
Tony Smalley Consulting, LLC
454 Seasons Drive
Grand Junction, CO 81503 USA
tony@tonysmalleyconsulting.com

Giuseppe Vannini, Ph.D.
GE Oil & Gas, Nuovo Pignone
Via Felice Matteucci, 2
50127 Florence, Italy
giuseppe.vannini@np.ge.com

Luc L. Vermin
Shell Petroleum Development Co.
of Nigeria, Ltd.,
P.O Box 263, Port Harcourt,
Rivers State, Nigeria
luc.l.vermin@shell.com

ABSTRACT

This paper documents the potential for excess distortion of a honeycomb damper seal under high differential pressure in a centrifugal compressor, the problems this can cause, and options for solution. A strong negative stiffness can result, dropping the first natural frequency into a region of negative effective damping. The paper shows the need to manage seal clearance profile and inlet swirl to avoid this condition, and to optimize damper seal contribution to stability. The paper presents predicted seal distortion, resulting dynamic characteristics, and their influence on rotor stability. Field vibration data confirm seal distortion under pressure can cause damaging, self-excited sub-synchronous vibrations, and that an appropriate seal clearance profile predictably corrects this condition. The paper shows that optimum stability requires uniquely different clearance profiles for low and high-pressure compressors.

KEY WORDS

Rotor dynamics, damper seal, divergence, centrifugal compressor

1 INTRODUCTION

Centrifugal compressors are widely used in oil and gas production. High stage counts, flexible rotors, high speeds and pressures make such applications prone to self-excited vibrations. Potential excitation sources include eye seals, balance piston and division wall seals, oil seals, and impellers. When a rotor deflects laterally, fluid forces from these sources have a "cross-coupling" component, which can excite whirling. Any tendency to whirl at a natural frequency also generates fluid damping forces, which oppose the whirl; instability occurs when net cross-coupling forces exceed net damping forces acting at the natural frequency.

Research has enhanced understanding of seal forces. Seal models and test data have shown how inlet pre-swirl in the rotation direction increases cross-coupling forces and aggravates instabilities. Shunt holes and swirl brakes have evolved as methods to control inlet swirl.

Damper seals have also evolved to control destabilizing forces: Memmott [1] describes the effective application of a honeycomb seals; Yu and Childs [2] describe hole pattern seals; Vance and Schultz [3] document the pocket damper seal. This paper focuses on the honeycomb seal, but Yu and Childs' work suggests the results will apply directly to hole pattern seals.

The honeycomb's surface array of small, six-sided holes machined normal to the stationary seal surface have depth several times the clearance. Kleynhans and Childs model [4] assumed an isothermal gas, but included the effect of the holes on the gas acoustic velocity, predicting dynamic coefficients, which closely match test data.

Although not free of cross-coupling, the honeycomb seal develops higher "effective damping" than a comparable labyrinth. "Effective damping" equals direct damping with cross-coupling stiffness, divided by angular frequency, subtracted. The "crossover frequency," at which the seal's effective damping drops to zero is lower than for other seals. With high effective damping and low crossover frequency, the honeycomb seal has widely replaced balance piston and division wall labyrinths in critical machines.

Moore, Walker, and Kuzdzal [5] describe a hole pattern seal with shunt holes, whose effective damping increases with differential pressure. Using a magnetic bearing to excite the rotor, they documented that this seal design causes system log decrement to increase with pressure.

Recent results show the significance of axial clearance variation in a honeycomb seal. Smalley, Camatti, Childs, Hollingsworth, Vannini, and Carter [6] demonstrated with tests and analysis that a linear clearance increase in the flow direction substantially increases maximum effective damping, but also creates a strongly negative, low frequency, stiffness. In a low-pressure application, they showed the benefit of increased damping more than offset the reduced stiffness, substantially increasing the rotor's predicted log decrement.

In 2003, Camatti, Vannini, Fulton, and Hoppenwasser [7] first showed that, for some medium to high pressure back-to-back compressors, the negative stiffness caused by a diverging clearance completely negates the benefits of higher maximum damping; it dropped the first natural frequency into a region of negative effective damping. The unplanned divergence resulted from division wall seal distortion under pressure, temperature, and centrifugal forces. The problem was discovered in a full load test and was solved by a redesigned converging honeycomb seal with shunt holes.

Tecza, Soulas, and Eldridge [8] demonstrate a probabilistic approach to managing manufacturing tolerance uncertainty in determining seal clearance profile.

Eldridge and Soulas [9] introduce a "Damper Seal Divergence Stability Threshold" and illustrate application to a straight through, six-stage, compressor (4.5:1 pressure ratio). The balance piston damper seal diverged under pressure and dropped the first natural frequency into a negative damping region. The solution again was to machine a converging clearance.

The present paper expands on the importance of managing seal axial clearance variation, with reference to the low and high pressure casings (both of back-to-back configuration) of a train to compress natural gas associated with oil production in the Niger Delta. It shows that, depending on the extent of distortion under pressure, a converging or diverging clearance can optimize stability of a honeycomb division wall seal. The train exhibited subsynchronous vibration of the high-pressure casing during commissioning, disrupting production and requiring an expedited, but assured, solution for both compressors. The HP compressor seal distorted enough to require a converging clearance honeycomb seal under undistorted conditions. The LP damper seal distorted negligibly under pressure, and its stability was safely optimized by designing for diverging clearance under both machined and operating conditions.

2 COMPRESSION TRAIN DESCRIPTION

The train is composed of two back-to-back compressors driven by a gas turbine through a speed increasing gearbox (Figure 1). The compressor, which experienced the high vibrations issue, was the high-pressure casing. Total train absorbed power is about 9 MW, the maximum continuous speed (MCS) is 10,059 RPM, and the total train pressure ratio is 48 (8 for the first casing and 6 for the second casing).

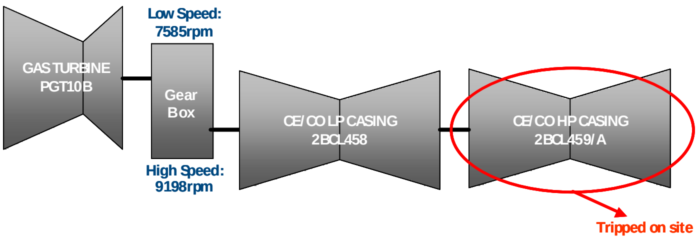

Figure 1: General Train Layout

The first casing connected to the gearbox is the low-pressure unit (LP). Since it is a back-to-back machine, it is composed of two sections: the gas flows in opposite directions through the two parts (from the end to the center) in order to better balance the thrust load and fit the maximum number of stages in a single casing. Both sections have four impellers. The journal bearings are tilting pads type, standard compressor manufacturer design. The thrust bearing is located inside the bearing span in order to minimize the overhung mass since this is a machine with two flexible couplings.

The original internal seal arrangement of the LP compressor contains a center balance piston with a tooth-on-stator labyrinth seal with shunt holes. The end balance piston seal is an abradable, tooth-on-rotor, labyrinth seal. The impeller shroud uses tooth-on-stator labyrinth seals with no swirl brakes.

The high-pressure unit (HP) is the final machine of the train, and it also has a back-to-back arrangement. The first section has four impellers, while the second section has five. The journal bearings are tilting pads type. The thrust bearing is located outside the bearing span, on the opposite side with respect to the flexible coupling.

The original internal seal arrangement of the HP compressor contains a honeycomb center balance piston seal without shunt holes. The end balance piston seal is an abradable, tooth-on-rotor labyrinth seal. The impeller shroud uses tooth-on-stator labyrinth seals with no swirl brakes.

The detailed design of the two compressors was performed in mid-2002, while the installation was performed only on end of 2004. Moreover, the design predated the most relevant manufacturer experiences in the field of damper seals negative stiffness (References 7, 8, 9), so it was based on the current rotordynamic design practices at that time.

Without going into great detail, both the units were located well within the manufacturer's experience envelope (see Figure 2), even though in the region of other critical machines due to their flexibility (LP unit) and mean gas density (HP unit). Due to this fact, the following were implemented at the time the units were originally built:

- Interstage honeycomb seal (HP unit).
- Shunt holes for interstage seal (LP unit).

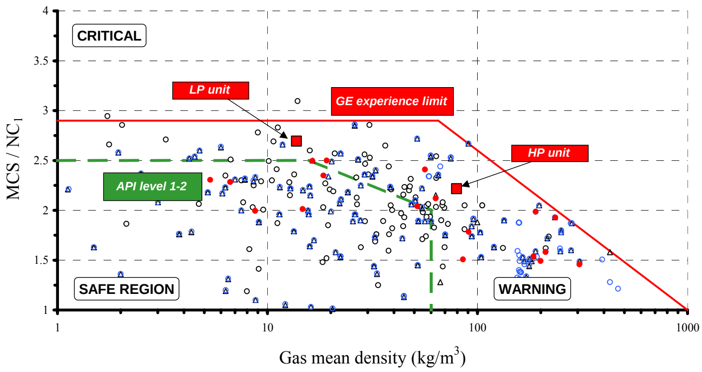

Figure 2: Fulton Diagram [10] with API 617 7th Edition and GE Limits

Finally, both the compressors underwent mechanical and thermodynamic tests in the manufacturer's factory (Figure 3) with satisfactory results (predictions in good agreement with measurements), but they had never been full load tested, and so the instability was not detected before the shipment and startup of the units.

Figure 3: Pictures of Compression Plant (left), Installed HP Unit (right)

3 FIELD OBSERVATIONS

When the compression train was commissioned, the HP compressor exhibited sudden high vibration that tripped the machine. The behavior was similar to a classic rotordynamic instability, where large subsynchronous vibration grows suddenly while loading the compressor but with several distinct differences.

Figure 4 shows a waterfall plot of the field startup of the HP compressor. The first sign of subsynchronous vibration (SSV) is a low level amount at about 12% of running speed. This low frequency component continued to grow to the point that a subsynchronous component appeared at about 40% of running speed, as indicated in the figure. This component

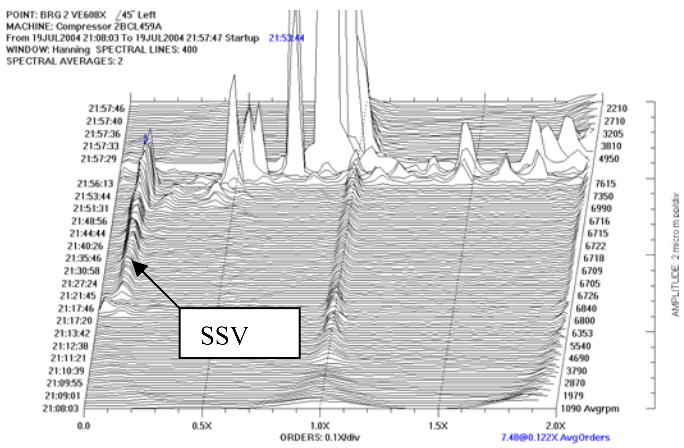

Figure 4: Waterfall Plot from Field Start-Up of HP Compressor

quickly grew resulting in very high vibrations. The frequency then increased and approached the synchronous frequency. This increase is attributed to rubbing of the honeycomb seal at the interstage diaphragm. This seal was acting like a third radial bearing, thereby, increasing the first natural frequency. The low frequency component near 12% of running speed is consistent with the first whirling mode that has dropped in frequency due to divergence of the honeycomb seal, as will be described later.

4 ROTORDYNAMIC MODELING

In order to predict the behavior of the current and modified configurations, a rotor dynamics model of the 9-stage HP compressor is generated. Comprising 74 stations it is derived from rotor drawings and shown in Figure 5. The honeycomb seal, located at the interstage diaphragm, is highlighted. Additional inertia is added to the shaft from couplings, dry gas seals, impellers, spacers, and balance drums. The LP model is similar except for 8 added impeller inertias, coupling inertias at both ends, and thrust bearing inertia inboard of the journal bearing.

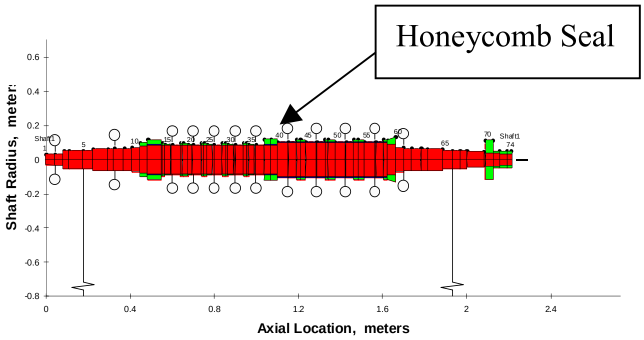

Figure 5: HP Compressor Rotor Dynamics Shaft Model

The rotor model was analyzed with the XLTRC[2] software developed at Texas A&M University's Turbomachinery Laboratory. This finite element code predicts undamped critical speeds, mode shapes, unbalance response, and damped natural frequencies (which provide stability information).

Bearing stiffness and damping characteristics were determined using the XLTRC[2] software. The software solves the two-dimensional Reynolds equation. The adiabatic option was used, with an 80% carry-over assumption, which implies 80% of the hot oil exiting one pad goes into the downstream pad. The remainder is made up by fresh oil supply. This approach provides reasonable correlation to the measured temperature from the factory test.

This software distinguishes synchronous and subsynchronous vibrations for tilting pad bearings. The code was used to provide a set of synchronous coefficients for unbalance response analysis and a set of subsynchronous coefficients for damped natural frequency and stability analysis. The particular features of the bearings (high preload, offset pivot) result in low frequency dependence of the resulting stiffness and damping coefficients.

5 ANALYSIS OF RESPONSE TO UNBALANCE

In order to predict the lateral vibration behavior, an unbalance response calculation is performed. This calculation utilizes an unbalance magnitude of 4 W/N (or 6,350 W/N), in accordance with API 617, 7th Edition guidelines, and shows the location of the rotor critical speeds. For the rotor weight (W) of 683 kg and a speed (N) of 10,059 RPM, evaluating 6,350 W/N yields 431 g-mm.

Figure 6 shows the response to 431 g-mm of unbalance applied at Station 39 of the HP rotor—at the interstage diaphragm location. The response corresponds to Probe 1, adjacent to the drive-end journal bearing. The display includes horizontal rotor vibration amplitude, vertical rotor amplitude, and the major axis of the elliptical response orbit. The first critical is strongly excited by this unbalance, exhibiting relatively light damping. Its peak response for both probes occurs between 4,060 and 4,070 RPM, as shown by the major axis of the elliptical orbit of response. This compares well to a measured value of 4,200 – 4,300 RPM from the factory mechanical test. The resonant amplitude of response to this unbalance excitation is just under 1.7 microns at Probe 1 and 2.6 microns peak-to-peak at Probe 2. Its peak amplitude is 14.3 microns at shaft center. The amplification factor based on the half-power points is about 6.1 and compares well to the measured value of 7.0 from the factory test.

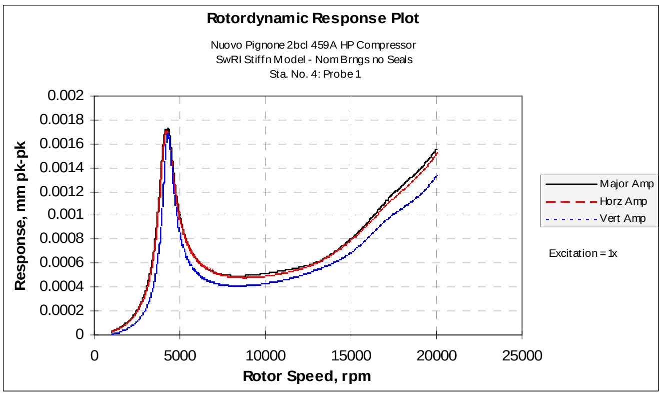

Figure 6: HP Probe 1 Response to 431 g-mm Unbalance at Center (1X API)

For the LP compressor, a similar peak response occurs between 3,540 and 3,560 RPM, with amplification factor between 5.2 and 6.4. With the unbalance weights at positions one-fourth of the way in from the ends, 180 degrees out of phase, the second critical speed is excited but lies well above maximum speed.

6 AERODYNAMIC EXCITATION AND SEAL ANALYSIS

To perform log decrement analysis and provide an assessment of stability, it is necessary to include potential destabilizing forces from the impellers and seals.

The labyrinth seals are also considered in the following stability analysis and utilized the XLLaby code from Texas A&M University. The impeller eye labyrinth seal of each impeller stage is included in the model, as well as the second section balance seal. The honeycomb seal at the center division wall is modeled using the code ISOTSEAL developed by Kleynhans and Childs [4]. This code has been well validated compared to test rig results [6].

Impeller excitation remains open to some controversy. The Wachel method [11] has been widely used since it was first developed, together with proposed variations; as one example the API 617, 7th edition [12] replaces the molecular weight in the original formulation with a constant value of 30 and replaces the density ratio across a section with the stage density ratio.

The original Wachel equation for aerodynamic cross-coupling (Q) is shown below. In recognition of the uncertainty with this calculation, values based on both the original Wachel formulation (referred to as "SwRI") and the API method are shown in this paper.

$$Q = 63,000 \frac{Mole \quad Weight}{10} \frac{Horsepower}{RPM \quad D \; b_3} \left(\frac{\rho_D}{\rho_S} \right) \tag{1}$$

D and b_3 are the impeller diameter and diffuser width, respectively, and ρ is the density at the suction and discharge of the compressor. The Q is calculated for each impeller and a modal summation is performed to obtain the equivalent value at the rotor center.

7 ROTOR DYNAMIC STABILITY ANALYSIS AND SEAL MODIFICATIONS CONSIDERED

The calculation of damped natural frequencies and associated log decrement provides a measure of rotor stability. Since the high vibration in the field was attributed to rotor instability, this analysis is the primary focus of this paper and uses the rotor model, the bearing analysis, the aerodynamic cross-coupling, and the seal analysis, described above. Table 1 summarizes two proposed modifications to the HP compressor. The original honeycomb seal's cylindrical bore deformed to a highly divergent condition under pressure and at temperature. The Rev. 1 modification machines a positive taper[1] into the seal cold, and under operation, a small divergence is expected. The seal deformation is greatly reduced by redesigning the seal carrier. Added shunt holes also reduce the swirl to an assumed value of 0.15. Swirl is defined by the ratio of the average circumferential velocity entering the seal divided by the local surface speed of the rotor. This value is based on experience modeling compressors with shunt holes. The Rev. 2 modification increased the average clearance and the amount of machined taper. For the labyrinth seals at the impeller eyes, swirl brakes were added, and the swirl is assumed to drop to a value of 0.25. This is a conservative value (high), since no CFD analysis was performed.

Table 1: Proposed Seal Modifications for HP Compressor

	Original	Rev. 1 Modification	Rev. 2 Modification
Honeycomb Seal	No Shunt (0.68 swirl) Zero Taper Cold clearance -0.494 mm Divergence in Operation	With Shunt (0.15 Swirl) 0.075 mm Cold Taper -0.05 mm Taper in Operation	With Shunt (0.15 Swirl) 0.09 mm Cold Taper 0 Taper in Operation 25% Larger Clearance
Eye Labyrinths	No De-swirl (0.68 swirl)	Swirl Brakes Added (0.25 swirl)	Swirl Brakes Added (0.25 swirl)

The original LP compressor design used a labyrinth seal. The Rev. 1 modification evaluated uses a honeycomb seal with a shunt, similar to the HP modifications. However, after review of the maximum rotor excursion at the first critical speed, the seal's radial clearance was increased. To obtain additional damping, divergence is machined into the seal. Shunt holes are added to reduce the swirl. The Rev. 2 modification increased the average clearance by about 50% and introduced an intentional divergence machined into the seal. For the labyrinth seals at the impeller eyes, swirl brakes were added. These changes are summarized in Table 2. There is no appreciable deformation of the LP interstage diaphragm seal due to the relatively low pressure.

[1] $taper = R^{seal}{}_{inlet} - R^{seal}{}_{outlet}$. Negative taper means divergent profile and vice versa.

Table 2: Proposed Seal Modifications for LP Compressor

	Original	Rev 1. Modification	Rev. 2 Modification
Interstage Diaphragm Seal	Tooth-on Stator Laby Seal No Shunt (0.68 swirl) Cyl. Cold Clearance	Honeycomb Seal With Shunt (0.15 Swirl) 0.0 mm Cold Taper -0.005 Taper in Operation	Honeycomb Seal With Shunt (0.15 Swirl) -0.05 mm Cold Taper -0.053 Taper in Operation 50% Larger Clearance
Eye Labyrinths	No De-swirl (0.68 swirl)	Swirl Brakes Added (0.25 swirl)	Swirl Brakes Added (0.25 swirl)

8 SEAL FINITE ELEMENT ANALYSIS

A two-dimensional finite element analysis (FEA) of the seal and interstage diaphragm assembly was performed to calculate the deformation of the seal assembly under pressure loading and the resulting change in radial clearance of the seal. Non-linear contact elements are used at the interface points between the different seal components to improve the accuracy of the prediction. These contact elements permit the contact between components that separate, more closely representing physical nature of the assembly. Figure 7 shows the original and hot/deformed clearance of the interstage diaphragm seal for the HP compressor. The analysis shows significant coning of the seal under pressure and temperature. The seal attachment design was modified to reduce the amount of seal deformation. Figure 8 shows the FEA results from this modified design. Notice the clearance starts with a convergent taper and results in a nearly straight clearance under pressure and temperature, with less deformation than the original design.

The analysis of the LP seal predicts only small amounts of divergent coning of the seal under pressure and temperature (less than 0.05 mm) using a similar modification as the HP compressor.

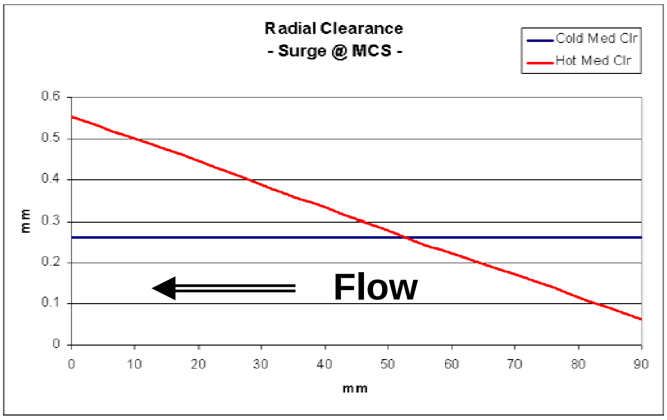

Figure 7: HP Compressor FEA Predicted Cold and Hot Clearance – Original Design

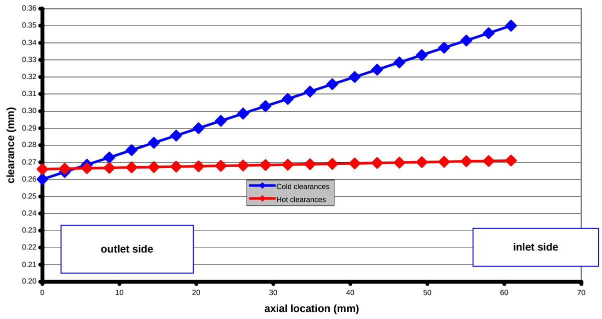

Figure 8: HP Compressor FEA Predicted Cold and Hot Clearance – Modified Design

9 STABILITY ANALYSIS – TRIP CONDITIONS

The first step in resolving the instability of the HP compressor is to attempt to predict the instability analytically using the exact field conditions when the unit went unstable. This approach validates the analytical approach and permits alternative designs to be evaluated. A pre-swirl ratio of 0.68 entering the impeller eye seal and the honeycomb seal was determined by calculating the swirl exiting the last impeller.

Table 3 is a summary table, which includes values of log dec and associated frequency for both an undeformed and deformed honeycomb seal using both levels of aerodynamic excitation (API and SwRI). The table shows a positive log decrement with no seal deformation, but with honeycomb (HC) seal deformation, the HP compressor is predicted highly unstable using either method for estimating the impeller excitation. The extreme reduction in frequency from 4,606 to 967 CPM as a result of honeycomb deformation should be noted. The low frequency vibrations in the site data prior to trip support this

Table 3: Summary of HP Stability Calculations for Trip Conditions

Run#	Deformation at HC?	Kxy-> (N/m)	API 6.15E+06	SWRI 8.01E+06
1	No	Log Dec->	0.192	0.138
		Freq->	4608	4616
2	Yes	Log Dec->	-11.47	-10.71
		Freq->	899	978

Table 4: Summary of LP Stability Calculations for Trip Conditions – Original Design

Run#	Deformation at HC?	Seal Divergence	Kxy->	API 1.86E+06	SWRI 1.91E+06
1	No	0	Log Dec->	0.058	0.056
			Freq->	3523	3523

prediction.

Table 4 summarizes a similar exercise for the LP compressor under the field conditions when the HP tripped and the LP compressor remained stable. Table 4 shows the LP compressor marginally stable using either impeller excitation and further validates the modeling approach.

10 STABILITY ANALYSIS – MAXIMUM CONTINUOUS SPEED (MCS) AND SURGE POINT

10.1 HP Compressor

Table 5 shows similar predictions at the maximum continuous speed (MCS) with operation near surge conditions (the highest pressure operating condition). Traditionally, this is considered the worst case operating point from stability considerations. Runs #1 and #2 represent the cold condition and hot/deformed seal condition, respectively. As expected, the original configuration shows the machine to be highly unstable at this speed and pressure, whatever the impeller excitation, even for the cold, undeformed condition. Notice how much the frequency drops for the deformed case, due to the large negative stiffness in the seal. This effect further reduces the log dec to a highly negative value.

Table 5: Summary of HP Stability Calculations for MCS/Surge Conditions – Original Design

Run#	Deformation at HC?	Kxy->	API 7.44E+06	SWRI 1.08E+07
1	No	Log Dec->	-0.297	-0.364
		Freq->	4677	4696
2	Yes	Log Dec->	-27.8	-25.7
		Freq->	883	957

Table 6 summarizes predictions for the first modification considered for the HP compressor (Rev. 1). Some convergence was machined into the seal, and other modifications reduced the amount of seal deformation under pressure. The results show stable behavior for both the original cold and the hot/deformed condition.

Table 6: Summary of HP Stability Calculations for MCS/Surge Conditions – Rev. 1 Modification

Run#	Deformation at HC?	Kxy->	API 7.44E+06	SWRI 1.08E+07
3	No	Log Dec->	0.897	0.843
		Freq->	6215	6220
4	Yes	Log Dec->	3.24	2.99
		Freq->	3114	3146
5	Yes+Toler.	Log Dec->		**-29.9**
		Freq->		**542**

However, a third case (Run #5) accounts for tolerance stack-up of both seal bore and all mating fits. With the resulting additional 0.12 mm of divergence the log dec becomes negative, showing the Rev. 1 design is sensitive to relatively small changes in seal clearance.

Table 7 presents results for the Rev. 2 modifications, in which the clearance was increased, and the machined taper was made more positive. This design is less sensitive to seal taper and tolerances. The log dec values for both levels of excitation are all positive. Run #9 shows the results with the seal clearance of all labyrinths and the honeycomb doubled. The log dec reduces but still remains well above 0.2 for both impeller excitation levels. Run #10 shows the predicted log dec with no seal effects to be stable with zero aero excitation (0.187 log dec), but unstable with small amounts of excitation. This emphasizes the positive influence of the honeycomb seal in maintaining a stable design. Additional runs with minimum and maximum bearing clearance show no significant change from the nominal bearing case.

Table 7: Summary of HP Stability Calculations for MCS/Surge Conditions – Rev. 2 Modification

Run#	Deformation at HC?	Kxy->	API 7.44E+06	SWRI 1.08E+07
6	No	Log Dec->	0.93	0.87
		Freq->	6035	6040
7	Yes	Log Dec->	1.25	1.17
		Freq->	5324	5331
8	Yes+Toler.	Log Dec->	2.13	1.94
		Freq->	3450	3475
9	Yes, 2X Clear	Log Dec->	0.53	0.46
		Freq->	5373	5378
10	No Seals	Log Dec->	-0.08	-0.20
		Freq->	4297	4307

Figure 9 compares the three HP configurations, using the hot and deformed results in a stability map (which plots the calculated log dec versus applied cross-coupled stiffness at the rotor mid-span). A threshold cross-coupling value occurs where log decrement changes sign. The ratio of this threshold cross-coupling to the API excitation, termed the "stability margin", will be discussed below as a measure of stability.

Figure 9 shows a large negative log dec (unstable) for the original configuration, resulting from the divergence of the honeycomb seal at the interstage diaphragm. The Rev. 1 modification greatly improves the log dec by eliminating most of the

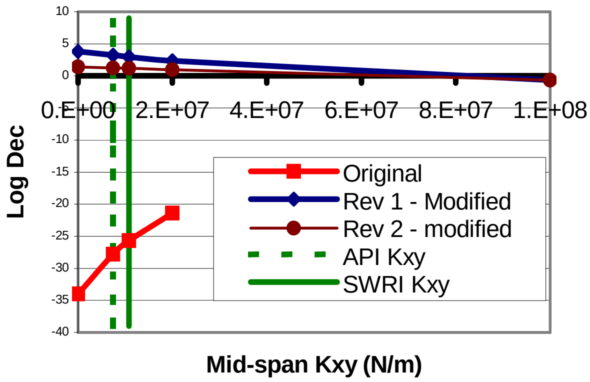

Figure 9: HP Stability Map with Proposed Seal Modifications

divergence in the seal. The Rev. 2 design shows a lower but positive log decrement compared to Rev. 1 and can accommodate a similar amount of cross-coupled stiffness. Its stability margin of over nine indicates a very stable machine. This verification adds a further safety margin to the selected honeycomb solution, which shows its robustness through the following sensitivity analysis. Figure 10 compares the predicted log dec for the two solutions considered as a function of seal taper, where a positive taper is a convergent clearance and a negative taper is divergent. The plot clearly shows how sensitive the Rev. 1 design is to seal taper. With slightly more divergent taper than the hot running condition, the log decrement quickly drops to a negative value because the negative stiffness generated by the divergent seal drops, the first natural frequency to the point where the effective damping goes negative. The Rev. 2 design avoids this "cliff".

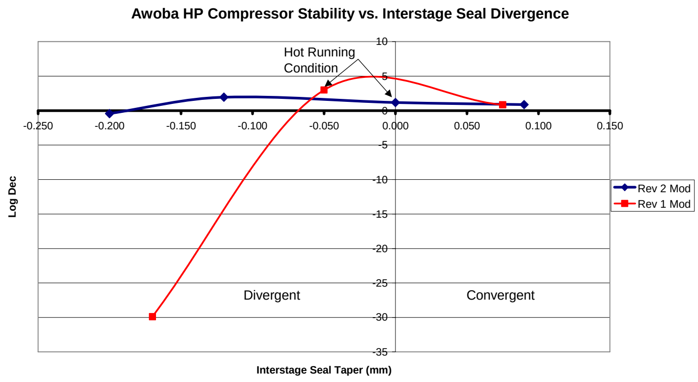

Figure 10: HP Sensitivity to Seal Taper

10.2 LP Compressor

Table 8 shows the original LP configuration predicted unstable at the MCS/Surge condition. Only the un-deformed case is shown since the amount of deformation is minimal. Even though the LP unit did not go unstable during part-load operation, these predictions indicate the potential for instability at full load.

A sensitivity study on the effect of divergence shows stable behavior for moderate levels of divergence, but the system goes unstable for divergence values greater than 0.13 mm with rev 1.

Table 9 shows that the Rev. 2 modification, with the clearance opened up and additional machined negative taper (divergence), is less sensitive to manufacturing tolerances and divergence. The four seal cases considered are cold, hot/deformed, hot/deformed with tolerance, and nominal seal clearance doubled. All log dec values for both levels of excitation are above 0.2, except with seal clearance doubled, for which log dec still remains positive.

Table 8: Summary of LP Stability Calculations for MCS/Surge Conditions – Original Design

Run#	Deformation at HC?	Seal Divergence	Kxy->	API 2.09E+06	SWRI 3.30E+06
1	No	0	Log Dec->	-0.182	-0.233
			Freq->	4677	4696

Table 9: Summary of LP Stability Calculations for MCS/Surge Conditions – Rev. 2 Modification

Run#	Deformation at HC?	Seal Taper	Kxy->	API 2.09E+06	SWRI 3.30E+06
1	No	-0.05	Log Dec->	0.231	0.184
			Freq->	3524	3525
2	Yes	-0.053	Log Dec->	0.259	0.211
			Freq->	3495	3496
3	Yes+Toler.	-0.173	Log Dec->	0.367	0.308
			Freq->	3173	3175
4	Yes, 2X Clear	-0.106	Log Dec->	0.176	0.13
			Freq->	3543	3543
5	No Seals		Log Dec->	0.055	0.01
			Freq->	3620	3620

It is emphasized that intentional divergence is machined into the honeycomb seal for the LP compressor, giving higher damping at the expense of some negative stiffness. With much lower operating pressures than for the HP compressor, the negative stiffness causes an insignificant drop in the natural frequency.

Run #5, which ignores seal effects, clearly shows that the honeycomb seal has a stabilizing influence rather than the previous destabilizing influence with the original toothed labyrinth seal. Again, minimum and maximum bearing clearance results do not change significantly from the nominal bearing case.

Figure 11 compares the predicted log dec as a function of seal taper for the two LP compressor solutions considered and clearly shows the Rev. 1 design to be quite sensitive to taper. With slightly more divergence than the hot running condition, the log decrement quickly drops to a negative value - a similar "cliff" to the Rev. 1 design of the HP compressor. With a larger clearance, the Rev. 2 design is much less sensitive to divergence and was the chosen design.

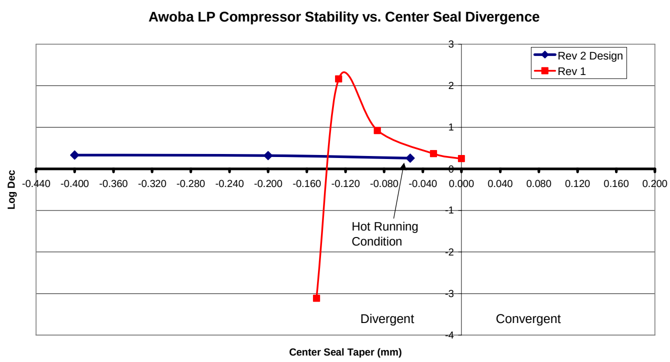

Figure 11: LP Sensitivity to Seal Taper

11 FIELD RESTART FOLLOWING SEAL MODIFICATION

Figure 12 shows the resulting waterfall plot of the HP compressor during the subsequent re-start. No sign of subsynchronous vibrations exists. The compressor was fully loaded over its entire operating map demonstrating good stability. The LP compressor also showed good stability over the range of operating conditions. The compression train was returned to normal service

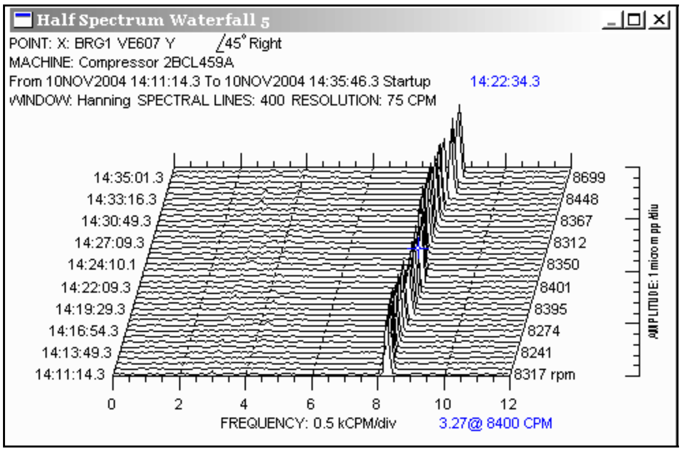

Figure 12: Waterfall Plot of HP Compressor Following Seal Modifications

12 END-USER'S VIEW

The rotordynamic instabilities as observed in the main centrifugal compressors of this project have caused significant loss of production and required many resources for rectification. The difficult logistics in the Niger Delta further complicated the recovery.

For any end user, but especially for one in this location and circumstance, compressor performance must be fully ascertained before the machine leaves the factory. It is noted that competition and the quest for better efficiency with fewer casings is driving the compressor manufacturers to inherently less stable designs. At the risk of conservatism, this author's company now restricts procurement to proven compressor design or demands an expensive and time consuming string test to full operating conditions.

The modeling of the complex rotors for the affected compressors and confirmation of the models by performance of the modified machines are building confidence that rotor dynamic behavior can be accurately predicted. Nevertheless, in view of the severe consequences in a very difficult environment, more confirmation is required before we will consider relaxing these design restrictions or string testing requirements.

13 CONCLUSIONS

A state of the art model was used to reliably predict centrifugal compressor stability accounting for the influences of damper seal distortion under load, and inlet swirl at labyrinth seals. Field data shows how these factors, unmanaged, can cause damaging instability, primarily when negative stiffness from diverging clearance profile in damper seals causes the natural frequency to drop into a region of negative effective damping. This field data and analysis show that managing the clearance profile of honeycomb seals and inlet swirl at eye seals can optimize the stability of low and high-pressure compressors. With significant seal profile distortion in high pressure units, the solution is to machine an offsetting convergent profile and set the mean clearance high enough that tolerances could not cause critical speed reduction into a negative damping region. With the low seal distortion in the low-pressure unit, a controlled diverging taper can optimize stability without risk of critical speed reduction into a negative damping region. Swirl brakes in the labyrinths and shunt holes in damper seals help minimize cross-coupling. With the clearance profile and swirl management, damper seals remain a powerful, wide-ranging tool for controlling centrifugal compressor stability.

ACKNOWLEDGEMENTS

The authors would like to thank the Nuovo Pignone team who worked hard to fix this critical field issue: Mr. Paolo Acciai who was actively involved in the seal redesign phase, Mr. Gabriele Fanti, Mr. Giuseppe Zaccaria, and Mr. Pietro Lo Martire, composing the team of service people who really made possible the restart of the compressors in such extreme environments. Finally, our appreciation goes to the management of Southwest Research Institute®, GE Oil & Gas Nuovo Pignone, and Shell Petroleum Development Company for their permission to publish this work.

REFERENCES

[1] Memmott, E. A., 1994, "Stability of a High Pressure Centrifugal Compressor through Application of Shunt Holes and a Honeycomb Labyrinth," Proc. of the 13th Machinery Dynamics Seminar CMVA, Toronto.

[2] Yu, Z. and Childs, D. W., 1998, "A Comparison of Experimental Rotordynamic Coefficients and Leakage Characteristics Between Hole-Pattern Gas Damper Seals and a Honeycomb Seal," ASME

Trans., Journal of Engineering for Gas Turbines and Power, Vol. 120, No. 4, pp. 778-783, October 1998.
[3] Vance, J. M. and Schultz, R. R., 1993, "New Damper Seal for Turbomachinery," Proceedings of the 14th Vibration and Noise Conference, ASME, Vibrations of Rotating Systems, 60, pp. 139-148.
[4] Kleynhans, G. and Childs, D. W., 1997, "The Acoustic Influence of Cell Depth on the Rotordynamic Characteristics of Smooth-Rotor/Honeycomb Stator Annular Gas Seals," ASME Trans. Journal of Engineering for Gas Turbines and Power, October 1997, Vol. 119, No. 4, pp. 949-957.
[5] Moore, J. J., Walker, S. T., and Kuzdzal, M. J., 2002, "Rotordynamic Stability Measurements During Full-Load Full-Pressure Testing of a 6000 PSI Reinjection Centrifugal Compressor," Proc. Thirty-First Turbomachinery Symposium, Turbomachinery Laboratory, Department of Mechanical Engineering, Texas A&M University, College Station, Texas.
[6] Smalley, A. J., Camatti, M., Childs, D. W., Hollingsworth, J. R., Vannini, G., and Carter, J. J., 2004, "Dynamic Characteristics of the Diverging Taper Honeycomb Seal," ASME 2004 Turbo Expo, Vienna, Austria, June 14-17, 2004.
[7] Camatti, M., Vannini, G., Fulton, J. W., and Hoppenwasser, F., 2003, "Instability of a High Pressure Compressor Equipped with Honeycomb Seals," Proc. of Thirty-Second Turbomachinery Symposium, Turbomachinery Laboratory, Department of Mechanical Engineering, Texas A&M University, College Station, Texas.
[8] Tecza, J., Soulas, T., and Eldridge, T., 2004 "Statistical Analysis of Damper Seal Clearance Divergence and Impact Upon Rotordynamic Stability," Presented at the 2004 International Mechanical Engineering Congress and Expo, Anaheim, CA, Nov. 13-20, 2004.
[9] Eldridge, T. and Soulas, T. A., 2005, "Mechanism and Impact of Damper Seal Clearance Divergence on the Rotordynamics of Centrifugal Compressors," Proceedings of GT2005 ASME Turbo Expo: Power for Land, Sea, and Air, June 6-9, 2005, Reno-Tahoe, Nevada USA.
[10] Fulton, J. W, 1984a, March 1984, "The Decision to Full Load Test a High Pressure Centrifugal Compressor in its Module Prior to Tow-Out," IMechE Second European Congress, Fluid Machinery for the Oil, Petrochemical and Related Industries,The Hague, The Netherlands.
[11] Wachel, J. C., and von Nimitz, W., (1980), "Assuring the Reliability of Offshore Gas Compression Systems," European Offshore Petroleum Conference and Exhibition, October 21-24, 1980, London, England, EUR 205.
[12] API 617, 7th Edition, (2002), "Axial and Centrifugal Compressors and Expander-Compressors for Petroleum, Chemical and Gas Industry Services."